Supporting Information for

A "turn-on" electrochemiluminescent biosensor for detecting mercury(II) at femtomole level based on the intercalation of $Ru(phen)_3^{2+}$ into ds-DNA

*Chun-Xia Tang, Yue Zhao, Xi-Wen He, and Xue-Bo Yin**

Research Center for Analytical Sciences,

College of Chemistry, Nankai University, Tianjin 300071, China

E-mail: xbyin@nankai.edu.cn

Contents:

S1. Experimental Section

S2. Intercalation of $Ru(phen)_3^{2+}$ into the ds-DNA

S3. Stability of two functional sections of oligonucleotide during the period for sensing Hg^{2+}.

S4. The stability of FO/$Ru(phen)_3^{2+}$ complex

S5. The electrochemical behavior of T_5-modified electrode in TPA solution

S6. Fig. S1-S5

S7. Table S1-S2

S1. Experimental Section

Apparatus. The electrochemical measurements for ECL emission were carried out on a Model LK98BII Microcomputer-based Electrochemical Analyzer (Tianjin Lanlike High-Tech Company, Tianjin, China). A traditional three-electrode system was used with Ag/AgCl/KCl (satured) as reference electrode, a 3-mm diameter Au disk modified electrode as working electrode, and Pt wire as counter electrode. The ECL emission was detected by using a model MPI-A Electrochemiluminescence Analyzer (Xi'An Remax Electronic Science & Technology Co. Ltd, Xi'An, China) at room temperature. The voltage of the PMT was set at -900 V in the detection process. The fluorescence is measured using an F-4500 spectrofluorometer (Hitachi, Japan) with a 1 cm quartz cell at room temperature.

Reagents. HPLC-purified DNA oligonucleotides were provided by Takara Biotechnology (Dalian, China) with the following sequences: 1: 5'-SH-$(CH_2)_6$-TTTTT-3' **(SS1)**

2: 5'-TTTTT *GTCCG TGGCT GGGCA GAAAC TGCCC AGCCA CGGAC*-3' **(SS2)**. The italic part can form intermolecular double strand as shown in Scheme 1 and is used for probe intercalation.

3: 5'- AAAAA-3' (**SS3)**

All oligonucleotides were diluted to 5 μM in TE buffer (10 mM Tris-HCl, 1 mM EDTA, pH 7.5) as single-stranded concentration. Tris(1,10-phenanthroline)ruthenium chloride hydrate ($Ru(phen)Cl_2 \cdot H_2O$) and tripropylamine (TPA) were obtained from Sigma-Aldrich, Shanghai, China. 2-Mercaptoethanol (MCE) used to block the active sits was obtained from Yangguang Yunneng Biotechnology Company, Tianjin, China. Saline solutions were prepared with $Mn(Ac)_2$, $Mg(NO_3)_2$, $Pb(NO_3)_2$, $Zn(Ac)_2$, $Cd(NO_3)_2$, $Fe(NO_3)_3$, $CaCl_2$, $Co(Ac)_2$, $Cu(NO_3)_2$, $AgNO_3$, and $Hg(NO_3)_2$. Milli-Q ultra-pure water was used in each experiment.

A series of water samples were collected locally and filtered thoroughly with a 0.2 μm membrane. 10 μL water samples were used to determine Hg^{2+} content and for recovery experiment.

Sensing Hg^{2+}. The procedure for the determination of Hg^{2+} ions using the ECL biosensor was presented in Scheme 1. The new gold electrode (3-mm in diameter) was polished with 0.3- and 0.05-μm

aluminum slurry and ultrasonicated with distilled water for 3 minutes. The electrodes were cleaned further in 0.1 M H_2SO_4 by potential scanning between -0.2-1.6 V until a remarkable voltammetric peak was obtained. The gold electrode was modified with SS-DNA (T_5, **SS1**) using 6 μL of 5 μM thiolated solution for 0.5 h at 36 °C. Then, 2-mercaptoethanol (MCE) was used to block the active sites for 0.5 h at 36 °C. At the same time, the functional oligonucleotide (10 μM) was mixed with 1 mM $Ru(phen)_3^{2+}$ for the probe intercalation at 4 °C in refrigerator over night for probe intercalation. 10 μM A_5 (**SS3**) was added into the functional oligonucleotide intercalated with $Ru(phen)_3^{2+}$ for the formation of A-T double helix structure for 1 h at 36 °C. 5 μL as-prepared functional oligonucleotide and 10 μL sample was dropped onto the **SS1**-modified electrode for 0.5 h at 36 °C. During this period, the T-Hg^{2+}-T construction formed and the probe, $Ru(phen)_3^{2+}$, was introduced into the electrode surface. After the modified electrode was cleaned thoroughly, the potential was scanned linearly from 0 to 1.25 V vs Ag/AgCl for the ECL determination of Hg^{2+} ions. The selectivity of the biosensor was tested in the presence of the competing metal ions such as Mn^{2+}, Mg^{2+}, Pb^{2+}, Zn^{2+}, Cd^{2+}, Fe^{3+}, Ca^{2+}, Co^{2+}, Ag^{+}, and Cu^{2+} at their 10 μM levels.

S2. Intercalation of $Ru(phen)_3^{2+}$ into the ds-DNA

The helical double-stranded DNA (ds-DNA) has the capacity to intercalate some small molecules into its grooves with high affinity. [S1-S3] Dong and co-workers [S3a] developed a fluorescence aptasensor using ethidium bromide as intercalator and fluorescent probe for thrombin determination. $[Ru(phen)_2(dppz)]^{2+}$ was intercalated into the double-stranded regions of the aptamer interacting to its target and was used to develop the electrochemical aptasensors for ATP and immunoglobulin G (IgG) by Fang's group. [S3b, c] Methylene blue, as electrochemical active probe, was intercalated into the aptamer probe in sandwich approach by using antibody and aptamer as capturing probe and detection probe, respectively. [S3d]

While $Ru(phen)_3^{2+}$ (phen=1,10-phenanthroline) and its derivatives can be intercalated into the grooves of ds-DNA, [S2, S3b, c] $Ru(phen)_3^{2+}$ has a high ECL emission efficiency. [S2a-d] Fluorescent experiment was previously used to evaluate site size and equilibrium constant between $Ru(phen)_3^{2+}$ and the ds-DNA. The calculated site size and equilibrium constant were 4 and $1.24 \times 10^4\ M^{-1}$, respectively. [S2a, S2b]

With the calculated site size of 4:1, every four bps can be intercalated with one $Ru(phen)_3^{2+}$ molecule. [S2a, S2b] Therefore, four $Ru(phen)_3^{2+}$ molecules intercalate into the double strand section of sixteen bps used in this work. Comparing with the probe molecule labelled chemically in the single site of a DNA sequence, this kind of intercalation provides a simple method to introduce the probe with high efficiency.

S3. Stability of two functional sections of oligonucleotide during the period for sensing Hg^{2+}.

Fluorescence experiments were used to investigate the stability of the FO/$Ru(phen)_3^{2+}$ complex. As shown in Fig. S1, the oligonucleotide largely enhanced the fluorescence of $Ru(phen)_3^{2+}$ (6003 vs. 2508 au) and the maximum emission wavelength also shifted from 584 to 589 nm due to its strong interaction to the adjacent DNA base pairs (Fig. S1b). [S2a, b] A fluorescence profile with the same intensity and maximum emission wavelength was observed after the FO/$Ru(phen)_3^{2+}$ complex formed the T-Hg^{2+}-T with Hg^{2+} (Fig. S1b against S1c). This suggests that the formation of the T-Hg^{2+}-T does not interfere with the intercalation of $Ru(phen)_3^{2+}$.

The effects on the ECL emission with and without the pre-formed hybrid between A_5 and the FO/$Ru(phen)_3^{2+}$ complex were also tested. As shown in Fig. S2, an obviously low ECL emission (612 vs 1025 counts) was observed if no the hybrid pre-formed for 1 nM Hg^{+} ions. Moreover, the reproducibility was poor. After analyzing the results, we found Hg^{2+} ions can also combine two FO via their Hg^{2+} identification sections and decrease the introduction of the FO/$Ru(phen)_3^{2+}$ complex into the electrode surface. However, if the Hg^{2+} identification section in FO/$Ru(phen)_3^{2+}$ complex formed the hybrid with a DNA single strand, A_5, The competitive binding leads to the high and reproducible ECL emission. The binding constant (K_b) of T-Hg^{2+}-T is 4.14×10^6 L mol $^{-1}$, which is higher than that of the A-T complex. [11] The competitive result makes Hg^{2+} ions is prone to hybridize the immobilized T_5 and the FO intercalated with $Ru(phen)_3^{2+}$ but not two FOs. Therefore, while the pre-formed A-T duplex in FO strand prevents the interaction between Hg^{2+} ions and two FOs, it does not affect coupling of the immobilized T_5 and the FO via Hg^{2+} ions (Fig. S2). Because $Ru(phen)_3^{2+}$ can be only intercalated into ds-DNA section, [12a, b] this intercalation does not affect the formation of T-Hg^{2+}-T. The results show that the Hg^{2+} identification section and probe intercalation section do not interfere with each other.

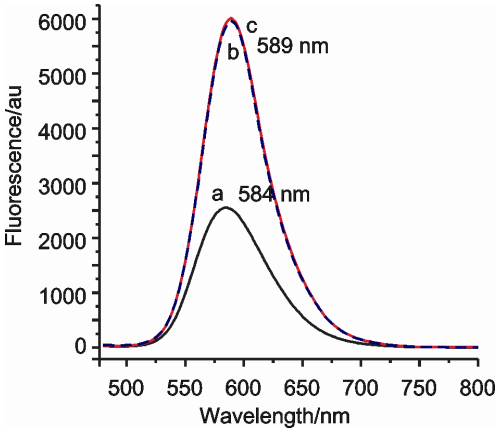

Fig. S1 Fluorescent profiles of (a) 10 μM free $Ru(phen)_3^{2+}$; (b) 10 μM $Ru(phen)_3^{2+}$ and 2.5 μM FO; and (c) 10 μM $Ru(phen)_3^{2+}$, 2.5 μM FO, 2.5 μM T_5, and 10 μM Hg^{2+}.

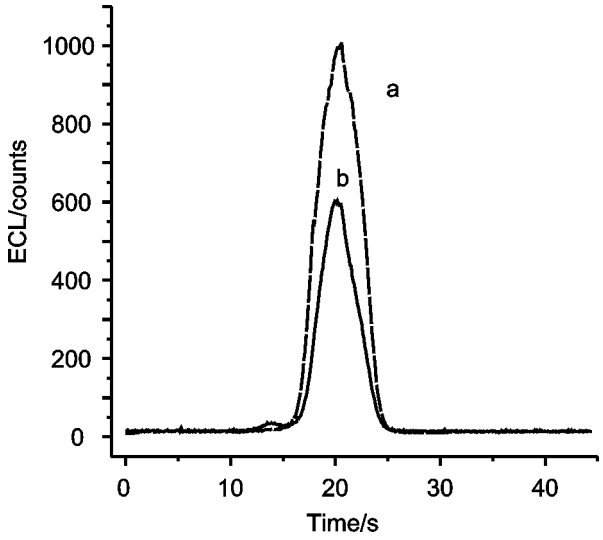

Fig. S2 The effects on the ECL emission with (a) and without (b) the pre-formed hybrid between A_5 and the FO/$Ru(phen)_3^{2+}$ complex for the determination of 1 nM Hg^{+} ions.

S3. The storage stability of FO/Ru(phen)$_3^{2+}$ complex

The functional oligonucleotide (FO, 10 μM) was mixed with 1 mM Ru(phen)$_3^{2+}$ for the probe intercalation at 4 °C in refrigerator over night. 10 μM A_5 (**SS3**) was then added into the FO intercalated with Ru(phen)$_3^{2+}$ for the formation of A-T double helix structure for 1 h at 36 °C. If the FO/Ru(phen)$_3^{2+}$ complex is stable enough for multiplex determinations, the analysis time can be shortened significantly. Its stability along with storage time with different storage modes was investigated. As shown in Fig. S3, if the FO/Ru(phen)$_3^{2+}$ complex is stored at 4 °C, the signal change is less than 5 % for the determination of 0.5 nM Hg^{2+} within three days although a decreased ECL emission is observed after being stored 10 days. However, if it is stored at -4 °C, a 50 % signal loss is observed after one day storage. It is possible that the construction of FO?Ru(phen)$_3^{2+}$ complex is changed after being frozen. Therefore, the FO/Ru(phen)$_3^{2+}$ complex was stored at 4 °C for the further work. Because the FO/Ru(phen)$_3^{2+}$ complex can be prepared previously and are stable at least 3 days, only the incubation time (30 min) for sample and FO/Ru(phen)$_3^{2+}$ complex on the electrode surface and the analysis time (less than 1 min) are taken for each assay with pre-prepared FO/Ru(phen)$_3^{2+}$ complex. Because the FO/Ru(phen)$_3^{2+}$ complex can be pre-prepared as shown in Fig. S3, the time taken for each assay only includes the incubation time (30 min) for sample and FO/Ru(phen)$_3^{2+}$ complex on the electrode surface and the analysis time (less than 1 min).

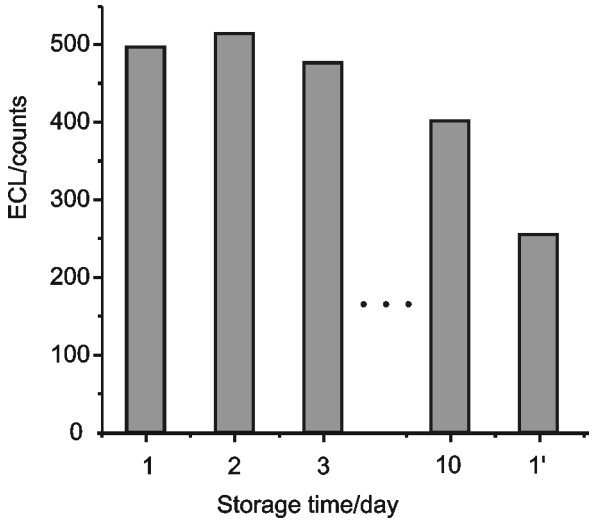

Fig. S3 The effect of storage time and mode (cold storage at 4 °C or freeze storage at -4 °C) of FO/Ru(phen)$_3^{2+}$ complex for 500 pM Hg^{2+} ions. 1, 2, 3, and 10 indicate the number of days for the storage at 4 °C and 1' is the number of days for the storage at -4 °C.

S4. The electrochemical behavior of T_5-modified electrode in TPA solution

Fig. S4 presents the CVs of PBS (pH 7.5) containing 20 mM TPA at the T_5-modified electrode with different scan rates. The anodic peak currents are directly proportional to the square root of the scan rates (Fig. S4B), indicating the diffusion-controlled TPA oxidation. Although a significantly improved anodic current for TPA oxidation was observed at the T_5-modified electrode, the currents were lower than those at the FO-modified electrode via the formation of T-Hg^{2+}-T at same scan rates. Moreover, no the peak related to $Ru(phen)_3^{2+}$ oxidation was observed (shown in Fig. 2). The previous work [S2b] indicated that ds-DNA strand can preconcentrate TPA via electrostatic interaction and provide an alkaline micro-environment to facilitate the deprotonation of TPA. Both of the two factors improve the oxidation of TPA significantly. The improved oxidation of TPA and the increased number of the probe molecules for single ds-DNA sequence achieve the sensitivity of the present mercury sensor over the single-site labelling to DNA strand.

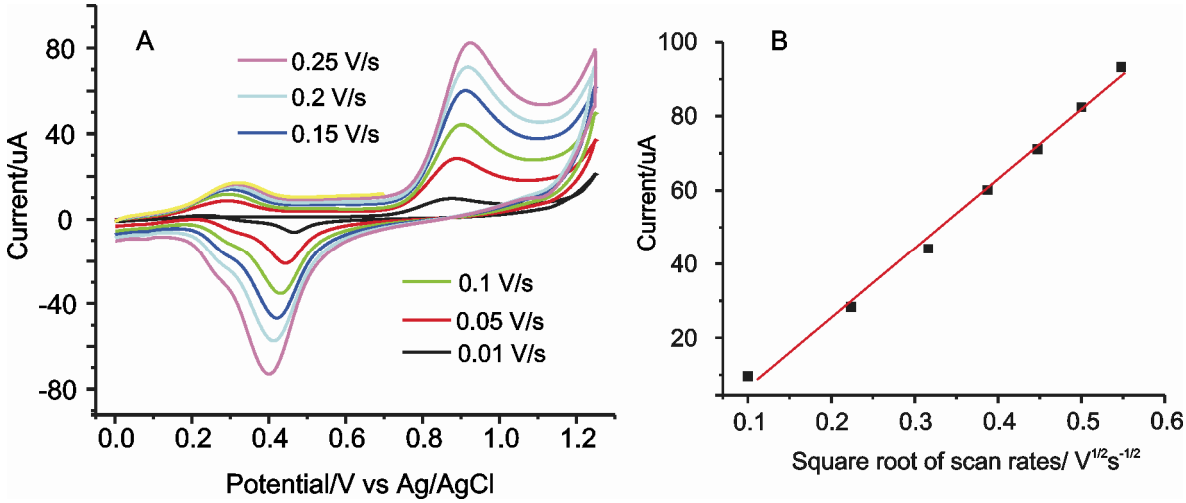

Fig. S4 (A) Cyclic voltammograms of the T_5 sequence modified Au electrode at different scan rate. (B) The relationship between the anodic peak currents and the square root of scan rates. Electrolyte: 0.1 M phosphate buffer solution (pH 7.5) containing 20 mM TPA.

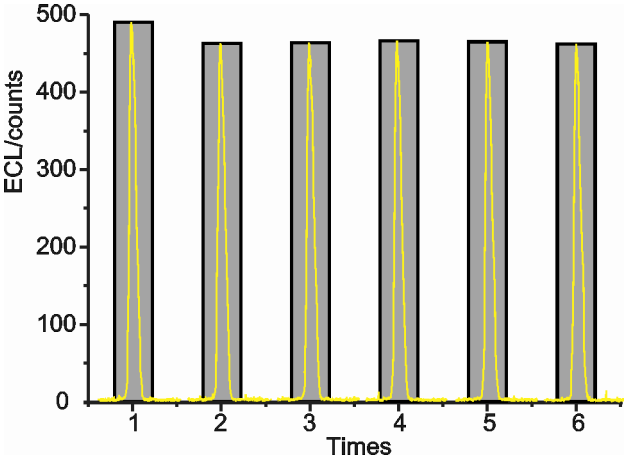

Fig. S5 The signal intensities and ECL profiles for six replicate determinations of 500 pM Hg^{+} ions with RSD of 2.1 %.

Table S1. Method detection limits (DLs) for Hg^{2+} ions using different oligonucleotide -based techniques.

Method	Notes	Sensing mode	DL/nM [b]	Ref.
ECL[a]	A functional oligonucleotide containing Hg identification section and ECL probe intercalation section	Turn-on	0.020	This work
ECL	$Ru(bpy)_3^{2+}$-doped silica nanoparticles labeled DNA	Turn-on	2.3	[S4]
Optics	Optical sensing with a conjugated polymer using its coupling to T-Hg^{2+}-T	Turn-on	42	[S5]
EC	The signal from Hg^{2+} reduced to Hg^{+} in combination with Au nanoparticle amplification	Turn-off	0.5	[S6]
FL [a]	Fluorescence from Au nanoparticles using the different electrostatic affinity between ss-DNA and ds-DNA	Turn-on	40	[S7]
FL [a]	Enhanced fluorescence from TOTO-3 intercalated into T-Hg^{2+}-T	Turn-on	0.6 ppb	[S8]
FL [a]	The formation of T-Hg^{2+}-T results in the quench to fluorophore	Turn-off	40	[S9]
FL	UO_2^{2+}-specific DNAzyme for the enhanced fluorescence	Turn-on	2.4	[S10]
FL	Simultaneous determination of Hg^{2+} and Ag^{+} by nucleic acid functionalized quantum dots.	Turn-off	10	[S11]
Colorimetry	The formation of T-Hg^{2+}-T inhibits the G-quadruplex DNAzyme activity	Turn-off	50	[S12]
Colorimetry	The formation of T-Hg^{2+}-T inhibits the G-quadruplex DNAzyme activity	Turn-off	4.5	[S13]
Colorimetry	The formation of T-Hg^{2+}-T inhibits the G-quadruplex DNAzyme activity	Turn-off	100	[S14]
Colorimetry	Hg^{2+}-induced aggregation of DNA-functionalized Au nanoparticles	Turn-on	250	[S15]
Colorimetry	The UV absorbance from the intermolecular four-stranded G-quadruplex–hemin complexes induced by Hg^{2+}	Turn-on	52	[S16]
Colorimetry	The UV absorbance from split G-quadruplex–hemin complexes induced by Hg^{2+}	Turn-on	19	[S17]
Colorimetry	Hg^{2+}-induced aggregation of DNA-functionalized Au nanoparticles	Turn-off	10	[S18]

[a] ECL: electrochemiluminescence; EC: electrochemistry; FL: fluorescence method.

[b] 1 nM corresponds to ca 0.2 ppb or 0.2 μg L^{-1}.

Table S2. Analytical results of Hg^{2+} ions in water samples with the present ECL biosensor.

	Added Conc. (nM)	Conc. Found (nM)	Recovery/%	By CV-AAS (nM) [a]
Tap water	0	n.d.[b]	--	n.d.
	1.00	1.04	104	--
Lake water	0	2.55	--	2.94
	1.00	3.57	102	--
	5.00	7.31	95.2	--
River water	0	1.70	--	1.80
	1.00	2.72	102	--
	5.00	6.84	103	--

[a] 10 mL of sample needed for each determination with CV-AAS, and only 10 μL needed for the present ECL biosensor.

[b] n.d. not detectable.

Supplementary References

[S1] a) N.C. Tansil, H. Xie, F. Xie, Z.Q. Gao, *Anal. Chem.* **2005**, *77*, 126-134. b) Z.Q. Gao, N.C. Tansil, *Anal. Chim. Acta* **2009**, *636*, 77-82. c) J. L. Wang, F. Wang, S. J. Dong, *J. Electroanal. Chem.* **2009**, *626*, 1-5. d) J.-G. Lee, K. Yun, G.-S. Kim, S. E. Lee, S. Kim, J.-K. Park, *Bioelectrochem.* **2007**, *70*, 228-234.

[S2] a) M. T. Carter, A. J. Bard, *Bioconjugate Chem.*, **1990**, *1*, 257-263. b) X. B. Yin, Y. Y. Xin, Y. Zhao, *Anal. Chem.* **2009**, *81*, 9299-9305. c) X. H. Xu, H. C. Yang, A. J. Bard, *J. Am. Chem. Soc.*, **1994**, *116*, 8386-8387.d) X. H. Xu, A. J. Bard, *J. Am. Chem. Soc.*, **1995**, *117*, 2627-2631. e) A. Mihailovic, I. Vladescu, M. McCauley, E. Ly, M. C. Williams, E. M. Spain, M. E. Nenez, *Langmuir* **2006**, *22*, 4699-4709. f) A. P. Xin, Q. P. Dong, C. Xiong, L. S. Ling, *Chem. Comm.* **2009**, 1658-1660. g) S. J. Wang, J. Milam, A. C. Ohlin, V. H. Rambaran, E. Clark, W. Ward, L. Seymour, W. H. Casey, A. A. Holder, W. J. Miao, *Anal. Chem.* **2009**, *81*, 4068-4075. h) Y. J. Sun, D. A. Lutterman, C. Turro, *Inorg. Chem.* **2008**, *47*, 6427-6434. i) D. A. Lutterman, A. Chouai, Y. Liu, Y. J. Sun, C. D. Stewart, K. R. Dunbar, C. Turro, *J. Am. Chem. Soc.* **2008**, *130*, 1163-1170.

[S3] a) B. L. Li, H. Wei, S. J. Dong, *Chem. Comm.* **2007**, 73-75. b) J Wang, Y. X. Jiang, C. S. Zhou, X. H. Fang, *Anal. Chem.* **2005**, *77*, 3542-3546. c) Y. X. Jiang, X. H. Fang, C. L. Bai, *Anal. Chem.* **2004**, *76*, 5230-5235. d) C. C. Huang, S. H. Chiu, Y. F. Huang, H. T. Chang, *Anal. Chem.* **2007**, *79*, 4798-4804.

[S4] X. Zhu, L. F. Chen, Z. Y. Lin, B. Qiu, G. N. Chen, *Chem. Commun.*, **2010,** *46*, 3149–3151.

[S5] X. F. Liu, Y. L. Tang, L. H. Wang, J. Zhang, S. P. Song, C. H. Fan, S. Wang, *Adv. Mater.* **2007***, 19*, 1471-1474.

[S6] Z. Q. Zhu, Y. Y. Su, J. Li, D. Li, J. Zhang, S. P. Song, Y. Zhao, G. X. Li, C. H. Fan, *Anal. Chem.* **2009***, 81*, 7660-7666

[S7] H. Wang, Y. X. Wang, J. Y. Jin, R. H. Yang, *Anal. Chem.* **2008**, *80*, 9021-9028.

[S8] C. K. Chiang, C. C. Huang, C. W. Liu, H. T. Chang, *Anal. Chem.* **2008**, *80*, 3716-3721.

[S9] A. Ono, H. Togashi, *Angew. Chem. Int. Ed.* **2004**, *43*, 4300-4302.

[S10] J. W. Liu, Y. Lu, *Angew. Chem. Int. Ed.* **2007***, 46*, 7587 –7590.

[S11] R. Freeman, T. Finder, I. Willner, *Angew. Chem. Int. Ed.* **2009***, 48*, 7818-7821.

[S12] T. Li, S. J. Dong, E. K. Wang, *Anal. Chem.* **2009***, 81*, 2144-2149.

[S13] N. Lu, C. Y. Shao, Z. X. Deng, *Analyst* **2009***, 134*, 1822-1825.

[S14] T. Li, B. L. Li, S. J. Dong, E. K. Wang, *Chem. Commun.* **2009**, 3551–3553.

[S15] C. W. Liu, Y. T. Hsieh, C. C. Huang, Z. H. Lin, H. T. Chang, *Chem. Commun.,* **2008,** 2242–2244.

[S16] D. M. Kong, J. Wu, N. Wang, W. Yang, H. X. Shen, *Talanta*, **2009**, *80*, 459-465.

[S17] D. M. Kong, N. Wang, X. X. Guo, H. X. Shen, *Analst*, **2010**, *135*, 545-549.

[S18] D. Li, A. Wieckowska, I. Willner, *Angew. Chem. Int. Ed.* **2008***, 47*, 3927-3931.